Journal of Physics: Conference Series

Effect of Detuning on Synchronization of Semiconductor Lasers

To cite this article: Hayder Abdulwahid Hammood and H. A. Sultan 2021 *J. Phys.: Conf. Ser.* **1963** 012109

2nd International Conference on Physics and Applied Sciences (ICPAS 2021) IOP Publishing
Journal of Physics: Conference Series **1963** (2021) 012109 doi:10.1088/1742-6596/1963/1/012109

Effect of Detuning on Synchronization of Semiconductor Lasers

Hayder Abdulwahid Hammood[1, 2]* and H. A. Sultan[1]**

[1]Physics Department, Education College for Pure Sciences, Basrah University, Basrah, Iraq.
[2]Education Department of Shatrah, Education Directorate of Thi-Qar, Thi-Qar, Iraq.

*h.a.hammood10@gmail.com
**hassabd67@yahoo.com

Abstract. A simulation of chaos-synchronization of unidirectionally open-loop master-slave configuration semiconductor lasers is introduced. We consider three scenarios, both lasers are single-mode, multi-mode lasers, with three modes where the interaction is between each mode of transmitter with the corresponding mode of the receiver, and the third scenario is for 5 modes. The simulation was focused on the influences of frequency-detuning of different values of coupling strength for two types of synchronization, anticipating synchronization (AS) and isochronous synchronization (IS). The simulation results demonstrate that scenarios are sensitive to the frequency-detuning between transmitter's and receiver's lasers. So, the suitable increasing of coupling strength is a necessary solution to decrease the frequency-detuning effect and saving synchronization with significantly broad high-quality, which means excellent feasibility.

1. Introduction

The synchronization phenomenon fundamentally describes the ability of a set of self-oscillators, to oscillate in unison due to their weak-interaction, to adjust their intrinsic rhythms [1]. In the 17th century, Huygens observed the synchronous motion, for the first time, in two maritime pendulum-clocks[2-4]. After that, synchronization has been observed in broad varieties of physical, chemical and biological systems[5]. One of these systems is communication applications[6,7], based on chaos to generate extremely complicated signals[8,9].

In recent years, optical-chaos based encryption schemes have attracted much attentions when compared with the traditional encryption methods[10], this momentum as a result of the requirement scenario and the pertinent technological progresses[11]. Generally, semiconductor-lasers (SCLs) are the most mainly used optical chaotic sources[7,12-14] due to their simplicity and low-cost[10]. They are commonly known for having complex and rich dynamical behavior intrinsically related to exciting physical properties and with the possible to drive to cutting edge applications[15]. The essential idea of secure-optical-communications is to employ chaotic output of transmitter to encode a data message and transfer to a receiver. Synchronizing transmitter-receiver is a fundamental condition so as to decode this message at receiver[16,17].

Buldú et al.[18] numerically demonstrated the emergence of two types of chaos-synchronization in two multimode scenarios, where they were consider, for simplicity, zero-detuning between the two lasers in each model. But this parameter, i.e. frequency-detuning, is an important influence on chaotic-synchronization performance of semiconductor-laser (SCL) systems, so, it should be taken into account[19]. Therefore, we theoretically study the effect of detuning on three scenarios. The 1st one, when the chaos-synchronization occurs between two single-mode lasers. The 2nd scenario is two multi-mode lasers, both 3 modes, where each mode of transmitter laser (TL) injected to the corresponding mode of receiver laser (RL). And the 3rd scenario is like the 2nd scenario except both lasers with 5 modes.

2. Modeling

We consider synchronization in SCL systems under effect optical-feedback (OF). The 1st scenario under study is shown in figure 1. It is presented two SCLs having nearly the same device features as light sources. The TL system with OF loop, which makes output TL oscillates as a chaotic. While the RL system without OF loop, as an open-loop system, with chaotic output injects only from TL to RL due to presence an optical isolator (OI). Under suitable conditions, RL may be synchronized with TL[20]. It can replace single-mode lasers in figure 1 with three-modes lasers or five-modes lasers to refer of 2nd scenario or 3rd scenario, respectively.

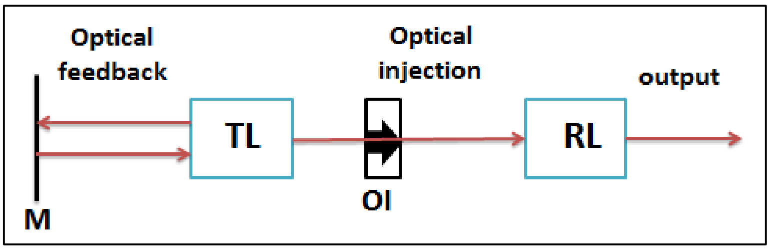

Figure 1. Synchronization scenario of two unidirectional coupled SCLs.

Many approaches used to generalize the single-mode Lang-Kobayashi model (LKM) in order to characterize the behavior of multi longitudinal modes of laser in the existence of feedback[21]. In this study, we will make develop of Buldú et al.[18] model of generalized LKM, to consider the effect of detuning on these scenarios, by the following set of equations for the evolution of the laser electric fields ($E_x(t)$) and the carrier density ($n(t)$).

$$\frac{dE_{(TL)x}}{dt}=\frac{1}{2}(1+i\alpha)[G_x(n_{(TL)})-\gamma]E_{(TL)x}(t)+k_M E_{(TL)x}(t-\tau_{(TL)})e^{-i\omega_{ox}\tau_{(TL)}}+\sqrt{2\beta n_{(TL)}}\zeta_{(TL)x}(t) \quad (1)$$

$$\frac{dE_{(RL)x}}{dt}=\frac{1}{2}(1+i\alpha)[G_x(n_{(RL)})-\gamma]E_{(RL)x}(t)+k_{S,x} E_{(TL)x}(t-\tau_{(RL)})e^{i\omega_{ox}\tau_{(RL)}+i\Delta\omega t}+\sqrt{2\beta n_{(RL)}}\zeta_{(RL)x}(t) \quad (2)$$

$$\frac{dn_{(TL,RL)}}{dt}=\gamma_e[cn_{th}-n_{(TL,RL)}(t)]-\sum_{x=1}^{m}G_x(n_{(TL,RL)})\left|E_{(TL,RL)x}\right|^2 \quad (3)$$

$$G_x(n)=\frac{g_c(n-n_0)}{1+s\sum_x\left|E_x(t)\right|^2}\left[1-\left(\frac{(x_c-x)\Delta\omega_l}{\Delta\omega_g}\right)^2\right] \quad (4)$$

Where x is the mode-number, $\xi_{(M,S)}(t)$ is Langevin noise forces to represent spontaneous emission and $G_x(n)$ is the gain-coefficient. Carrier noise is neglected. $P_x(t)=\left|E_x(t)\right|^2$ measures the number of photons. c is normalized, nth is the carrier number at the solitary-laser-threshold, given by cth=1 and threshold injection current $I_{th}=19.8mA$.

It is assumed, for all modes, TL feedback parameters k_M and feedback time ($\tau_{TL}=3.8ns$) to be equal, and the parameters α, γ and γ_e, for all modes to both SCLs, to be equal. $\omega_{ox}=\omega_c\pm(x_c-x)\Delta\omega_l$, where ω_c corresponding to the mode x_c. $\Delta\omega=2\pi\Delta f$, where Δf is the frequency-detuning. $\Delta\omega_l$ is the longitudinal mode spacing $\Delta\omega_l = 2\pi/\tau_l$. Coupling strength $k_{S,x}$ and coupling time $\tau_{RL} = 0$ are equal for all modes. Linewidth-enhancement-factor $\alpha = 2.5$ [4]. Other parameters are defined in table 1.

3. Results and discussion

With equations (1), (2) and (3) in hand, it is presently proceeding to measure the synchronization degree numerically under effect of detuning. The mechanism of chaotic synchronization is based on output oscillations of TL by optical feedback which injection unidirectional to RL.

We study the influence of frequency-detuning, from -40GHz to 40GHz, on the cross-correlations function with respect coupling strength, $20ns^{-1}$, $40ns^{-1}$ and $60ns^{-1}$, of all our scenarios. The cross-correlation function is determined to quantify the chaotic synchronization-quality, which is defined according to the following-equation[22]:

$$CCF(\Delta t) = \frac{\langle [P_t(t) - \langle P_t \rangle][P_r(t+\Delta t) - \langle P_r \rangle] \rangle}{\sqrt{\langle [P_t(t) - \langle P_t \rangle]^2 \rangle \langle [P_r(t) - \langle \mathrm{P}_r \rangle]^2 \rangle}} \tag{5}$$

Figure 2 presents the choatic-synchronization of the 1st scenario at $\Delta f = 0GHz\ and\ k_c = 20ns^{-1}$, it is noted that two types of synchronization appeared, AS and IS, between these single-mode lasers with very-good quality, CCF of AS and IS are (CCF=1.00) and (CCF=0.92), respectively. When we allow for a detuning with respect to the coupling strength in figure 3. It is observed by fitting the simulated that the curves which represent the quality of synchronization are decreasing with growth of frequency-detuning on both sides of zero-detuning, and the curves are increasing with the rising coupling strength, which agree with the refs. [20,23,24], although there are synchronization zones behind the non-synchronization zone, as in the curve at $k_c = 20ns^{-1}$ in the figure 3(a), it may be as a result of the complex behavior of lasers chaotic output. It also observed the area under the curve at $k_c = 60ns^{-1}$ remains larger than the area under the curve at $k_c = 40ns^{-1}$, which in turn is larger than the area under the curve at $k_c = 20ns^{-1}$. It can be seen that both types of synchronization, AS and IS, can wonderful appear until good values of detuning. Where synchronization at positive detuning is clearly better than synchronization at negative detuning, which agree with refs. [20,25] for both types of synchronization. There are deviation of the best synchronization toward positive detuning, which agree with ref. [25], for both types of synchronization, which made curves are not symmetric on both sides of zero-detuning.

Table 1. Simulation parameters [19,26].

Symbol	Definition	Value
$\mathbf{\Gamma}$	Cavity loss coefficient	0.238 ps^{-1}
$\mathbf{k_M}$	Feedback strength	$2 \times 10^{-2}\ ps^{-1}$
$\boldsymbol{\beta}$	Spontaneous emission rate	5×10^{-10} ps^{-1}
$\boldsymbol{\gamma_e}$	Carrier inverse lifetime	6.21×10^{-4} ps^{-1}
c	Injection current	1.015
$\boldsymbol{\tau_l}$	Internal round trip time	8.5ps
$\boldsymbol{\omega_c}$	Gain peak frequency	$\frac{0\ mod\ 2\pi}{\tau}$
$\boldsymbol{\Delta\omega_g}$	Material gain width	$2\pi \times 21.17$ THz
S	Saturation coefficient	1×10^{-7}
$\mathbf{g_c}$	Differential gain coefficient	3.2×10^{-9} ps^{-1}
$\mathbf{n_0}$	Transparency inversion	1.25×10^{8}

The choatic-synchronization of the 2nd scenario at $\Delta f = 0GHz\ and\ k_c = 60ns^{-1}$ is presented in figure 4. It is seen a very good AS and IS for all modes and total, which are (CCF=0.87) and (CCF=0.96) for mode 1, (CCF=0.53) and (CCF=1.00) for mode 2, (CCF=0.81) and (CCF=0.95) for mode 3, (CCF=0.74) and (CCF=0.96) for total, respectively. The effect of detuning on each mode and total of the 2nd scenario in figure 5. At which point, the curves fitting ebb away with growth detuning, and they increase with rising k_c, Except the curve in figure 5(3b), where curves increase visibly only when the rising between two values of k_c is $(40ns^{-1})$, It also showed synchronization zones behind the non-synchronization zone as shown in figure 5(3a), which agree with ref. [19]. It may be as a result of the complex behavior of lasers chaotic output which makes it difficult to predict its magnitude. The results are close to each others of all modes and total at each value of k_c for each type of synchronization and both sides of zero-detuning, which makes results more reliable. It is important to refer that both types of synchronization can appear until, relatively, high values of detuning. From these results, in addition to increasing curves with increasing k_c, it is also noted that positive detuning synchronization is better than negative detuning synchronization for both types of synchronization. The curves are not symmetric on both sides of zero-detuning because the deviation of the best synchronization toward positive detuning for both types of synchronization.

When we examine the effect of frequency-detuning on the cross correlations of 3rd scenario in figure 6. It is found that both types of synchronization of this scenario recorded all the features which is seen in 2nd scenario. So, there is agreement between them.

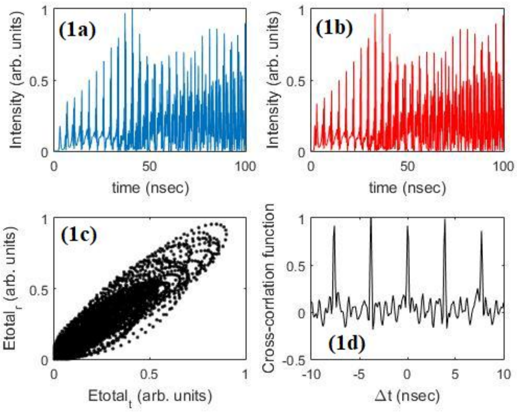

Figure 2. Synchronization of single-mode lasers at $\Delta f = 0GHz\ and\ k_c = 20ns^{-1}$. (1a) chaotic-output of TL with time. (1b) chaotic-output of RL with time. (1c) synchronization plot between TL and RL. (1d) the time shift CCF for TL with RL.

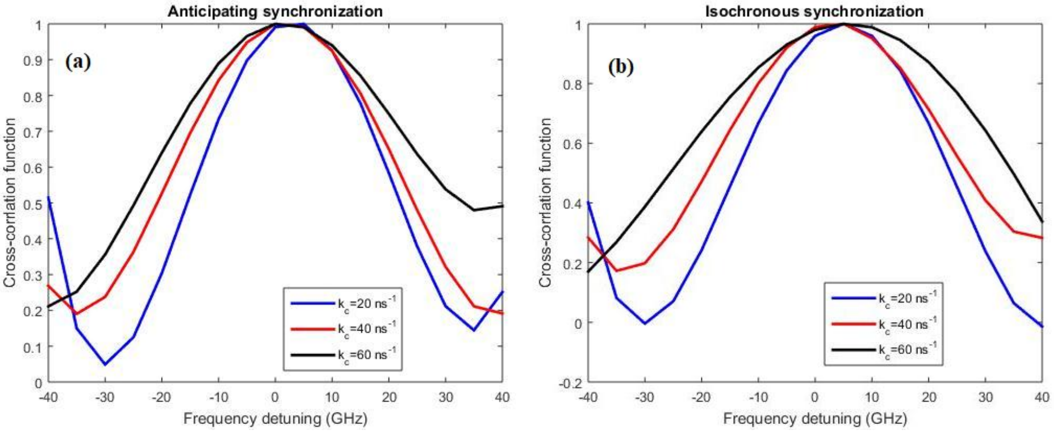

Figure 3. The curves fitting between CCF and frequency-detuning with respect coupling strength of single-mode lasers. (1a) Anticipating synchronization. (1b) Isochronous synchronization.

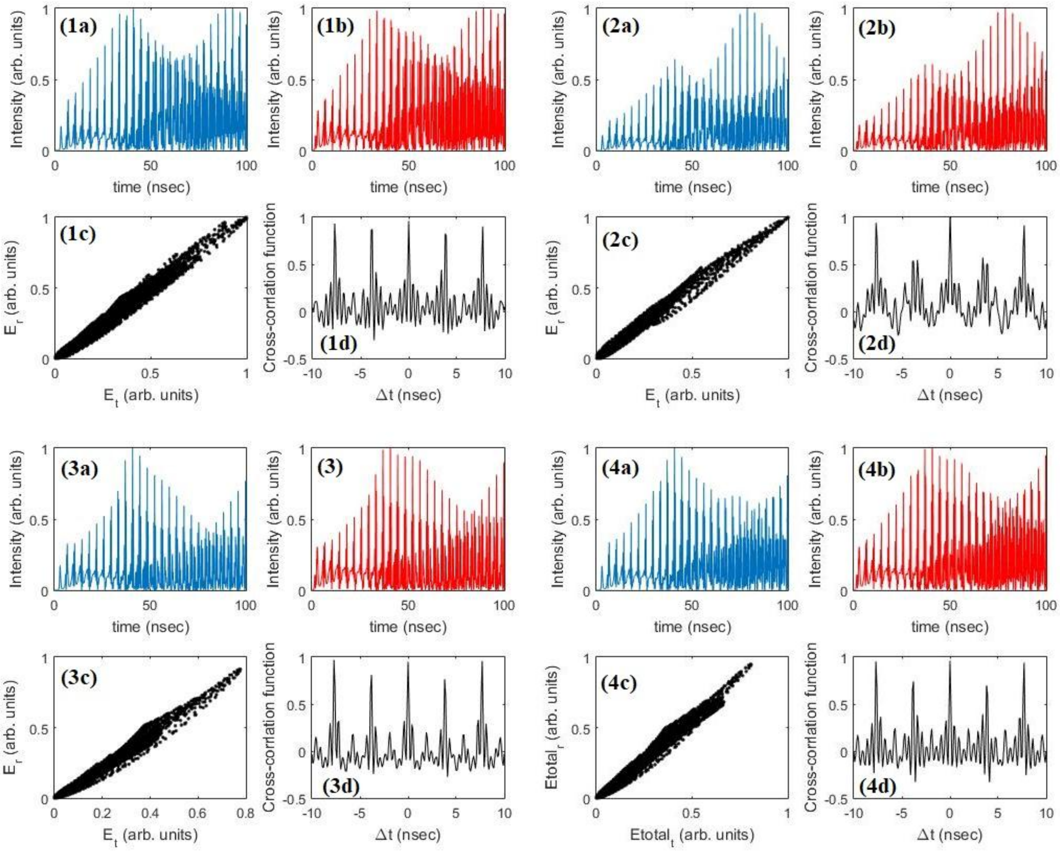

Figure 4. Synchronization of three-mode lasers at $\Delta f = 0GHz\ and\ k_c = 60ns^{-1}$ (1a, 2a, 3a and 4a) chaotic-output of modes 1, 2, 3 and total of TL, respectively, with time. (1b, 2b, 3b and 4b) chaotic-output of modes 1, 2, 3 and total of RL, respectively, with time. (1c, 2c, 3c and 4c) synchronization plot between of modes 1, 2, 3 and total of TL and RL, respectively. (1d, 2d, 3d and 4d) the time shift CCF for modes 1, 2, 3 and total of TL with RL, respectively.

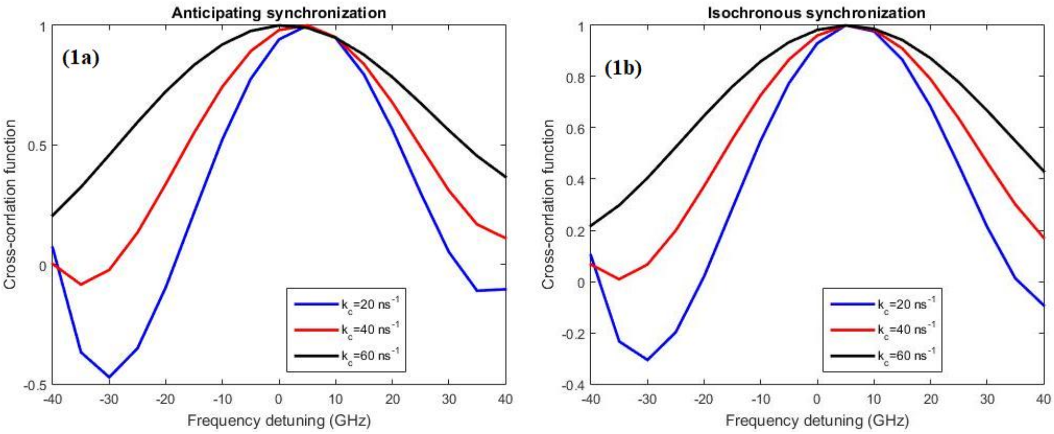

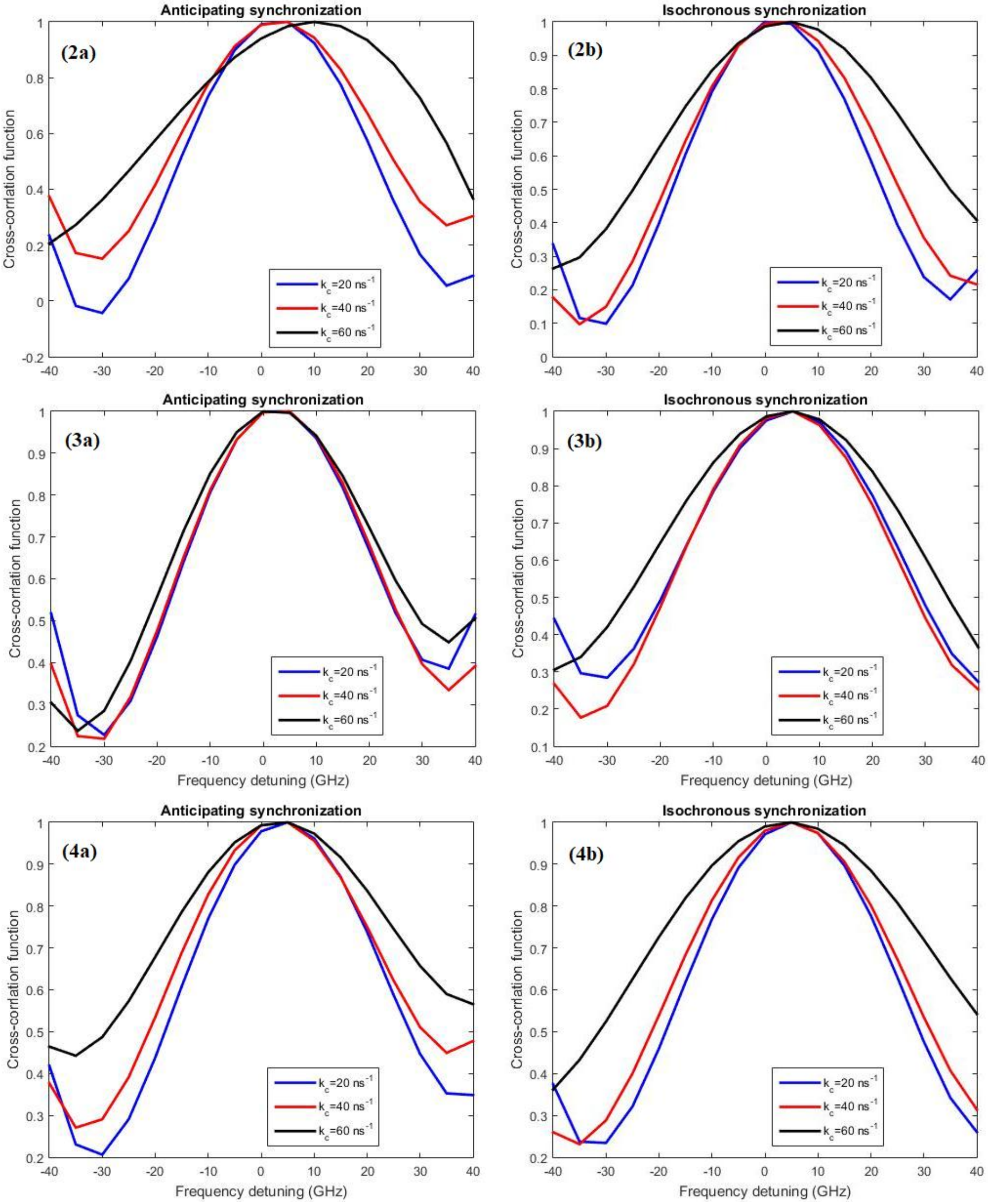

Figure 5. The curves fitting between CCF and frequency-detuning with respect coupling strength of multi-mode lasers (both with 3 modes). (1a, 2a, 3a and 4a) Anticipating synchronization of modes 1, 2, 3 and total, respectively. (1b, 2b, 3b and 4b) Isochronous synchronization of modes 1, 2, 3 and total, respectively.

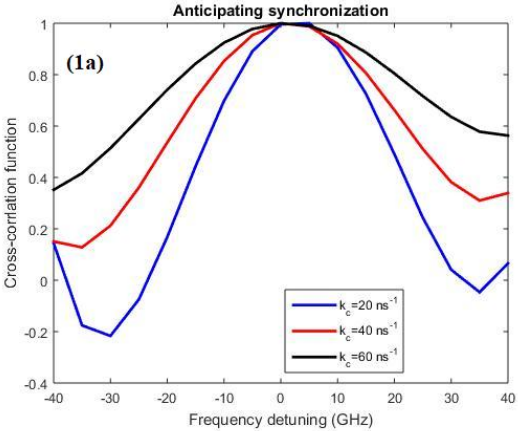
Anticipating synchronization
(1a)
Cross-corrlation function
1
0.8
0.6
0.4
0.2
0
-0.2
-0.4
-40 -30 -20 -10 0 10 20 30 40
Frequency detuning (GHz)
k_c=20 ns^-1
k_c=40 ns^-1
k_c=60 ns^-1

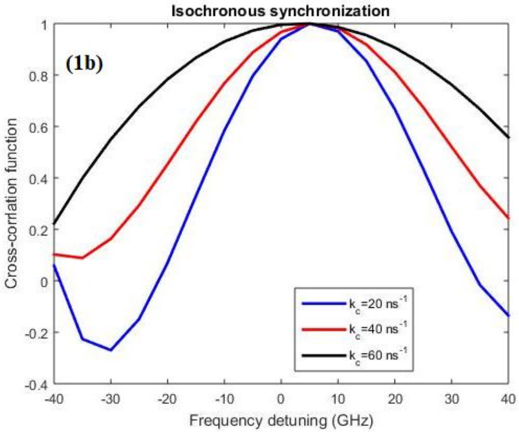
Isochronous synchronization
(1b)
Cross-corrlation function
1
0.8
0.6
0.4
0.2
0
-0.2
-0.4
-40 -30 -20 -10 0 10 20 30 40
Frequency detuning (GHz)
k_c=20 ns^-1
k_c=40 ns^-1
k_c=60 ns^-1

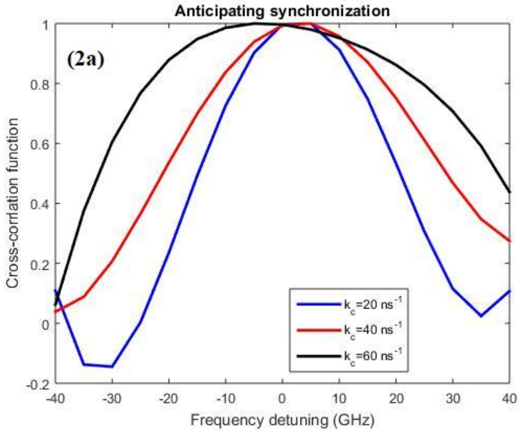
Anticipating synchronization
(2a)
Cross-corrlation function
1
0.8
0.6
0.4
0.2
0
-0.2
-40 -30 -20 -10 0 10 20 30 40
Frequency detuning (GHz)
k_c=20 ns^-1
k_c=40 ns^-1
k_c=60 ns^-1

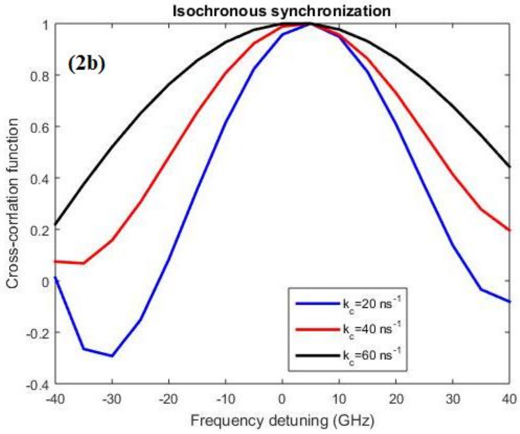
Isochronous synchronization
(2b)
Cross-corrlation function
1
0.8
0.6
0.4
0.2
0
-0.2
-0.4
-40 -30 -20 -10 0 10 20 30 40
Frequency detuning (GHz)
k_c=20 ns^-1
k_c=40 ns^-1
k_c=60 ns^-1

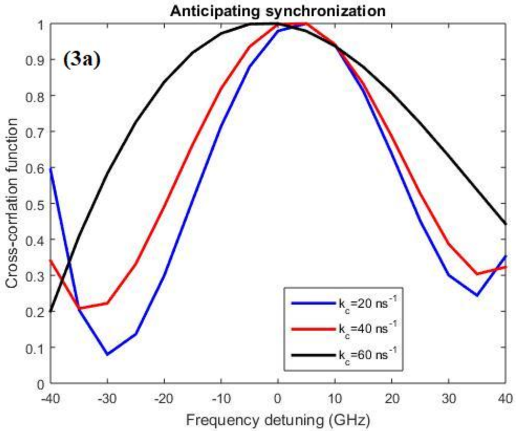
Anticipating synchronization
(3a)
Cross-corrlation function
1
0.9
0.8
0.7
0.6
0.5
0.4
0.3
0.2
0.1
0
-40 -30 -20 -10 0 10 20 30 40
Frequency detuning (GHz)
k_c=20 ns^-1
k_c=40 ns^-1
k_c=60 ns^-1

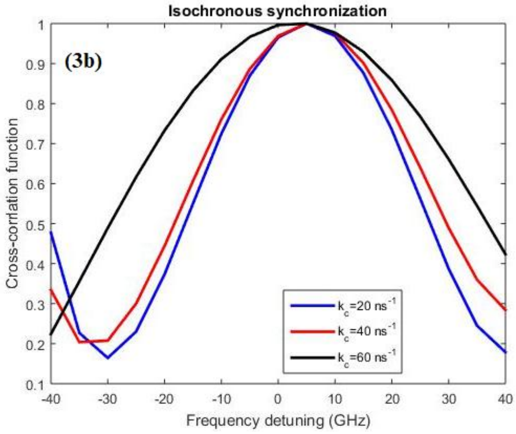
Isochronous synchronization
(3b)
Cross-corrlation function
1
0.9
0.8
0.7
0.6
0.5
0.4
0.3
0.2
0.1
-40 -30 -20 -10 0 10 20 30 40
Frequency detuning (GHz)
k_c=20 ns^-1
k_c=40 ns^-1
k_c=60 ns^-1

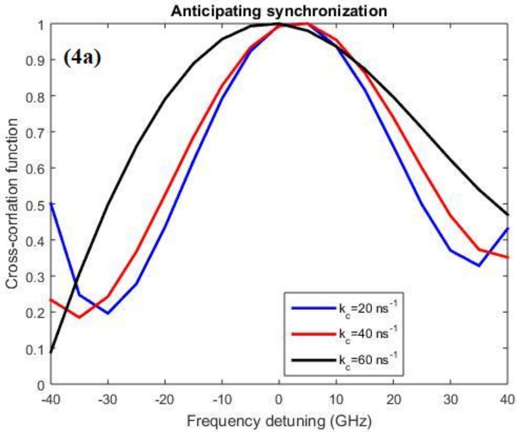
Anticipating synchronization
(4a)
Cross-corrlation function
1
0.9
0.8
0.7
0.6
0.5
0.4
0.3
0.2
0.1
0
-40 -30 -20 -10 0 10 20 30 40
Frequency detuning (GHz)
k_c=20 ns^-1
k_c=40 ns^-1
k_c=60 ns^-1

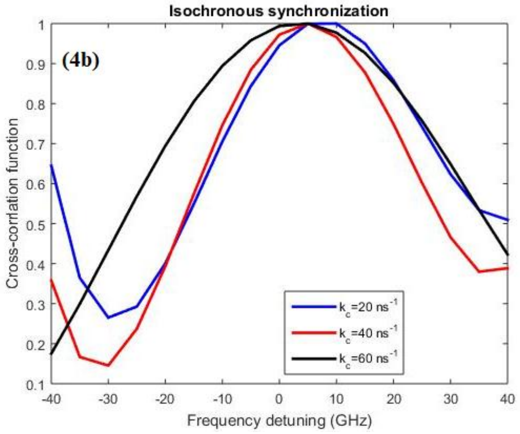
Isochronous synchronization
(4b)
Cross-corrlation function
1
0.9
0.8
0.7
0.6
0.5
0.4
0.3
0.2
0.1
-40 -30 -20 -10 0 10 20 30 40
Frequency detuning (GHz)
k_c=20 ns^-1
k_c=40 ns^-1
k_c=60 ns^-1

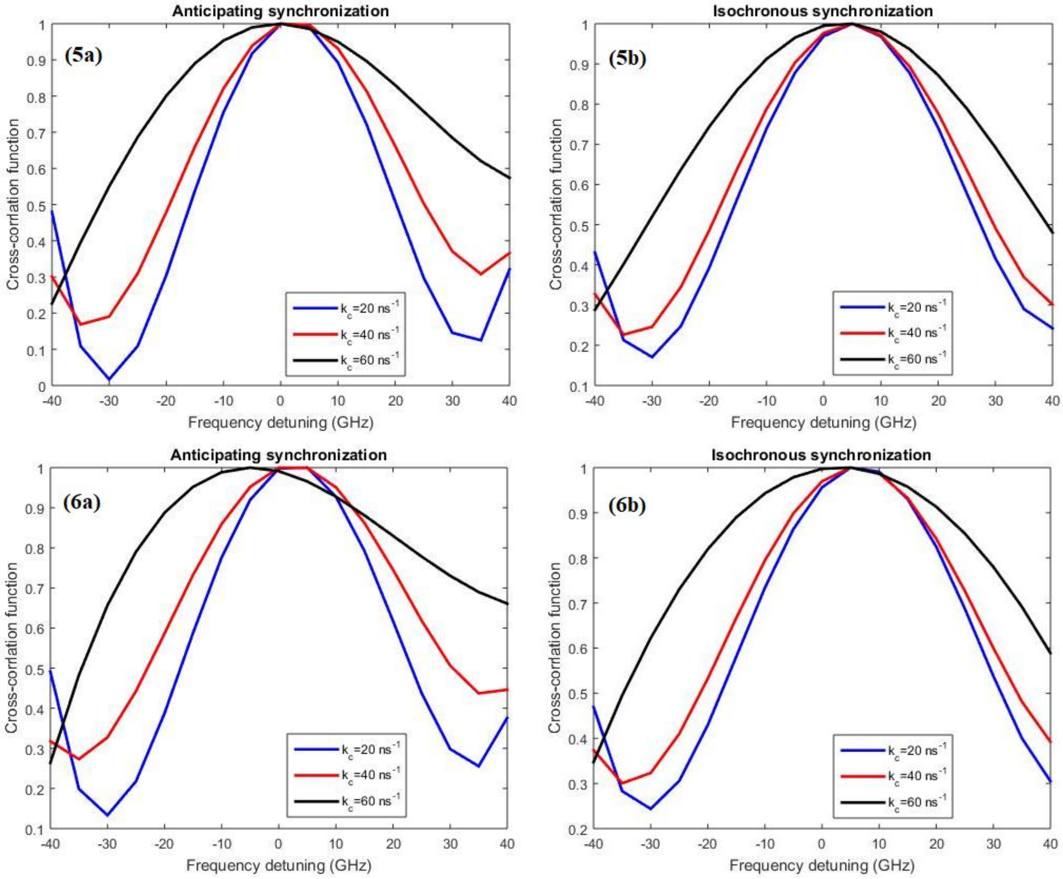

Figure 6. The curves fitting between CCF and frequency-detuning with respect coupling strength of multi-mode lasers (both with 5 modes). (1a, 2a, 3a, 4a, 5a and 6a) Anticipating synchronization of modes 1, 2, 3, 4, 5 and total, respectively. (1b, 2b, 3b, 4b, 5b and 6b) Isochronous synchronization of modes 1, 2, 3, 4, 5 and total, respectively.

4. Conclusion

The detuning-frequency effect on of three chaotic synchronization scenarios were studied via numerical simulation for single-mode scenario, three-mode scenario and five-mode scenario. For all these scenarios, It is appeared two types of synchronization, AS and IS. It is demonstrated that these two types of chaos-synchronization is decreasing with increasing frequency-detuning. Both types of synchronization may be obtained even if the certain-level of frequency-detuning exists, as long as k_c is large enough. It is found that both types of synchronization can obtained in the total output at CCF=0.5 for both sides of detuning, with excellent agreement between these three scenarios. The synchronization of positive-detuning is better than negative-detuning for both types of synchronization, which makes the deviation of the best synchronization toward positive-detuning for both types of synchronization, thus, The curves are not symmetric on both sides of zero-detuning. Therefore, k_c should be much larger at negative-detuning. Finally, the results of these three scenarios support each other, which makes them more reliable.

5. References

[1] Kumari N and Dwivedi S 2020 *Reson. – J. Sci. Educ.* **25** 539–565.
[2] Shimizu D and Okada T 2021 *Frontiers in Psychology* **12** 635534.
[3] Tanasijević I and Lauga E 2021 *Phys. Rev. E* **103** 022403.
[4] Sultan H A, Al-temimi K A, Ahmed A R and Emshary C A 2013 *J. Basrah Res.* **39** 13–27.

[5] Toiya M, González-Ochoa H O, Vanag V K, Fraden S and Epstein I R 2010 *J. Phys. Chem. Lett.* **1** 1241–1246.
[6] Abd Ali R H, Ghalib B A and Abdoon R S 2019 *7th Int. Conf. on Applied Science and Technology (ICAST 2019)* (Karbala: Iraq/AIP Conf. Proc.) **2144** 030012.
[7] Abd Ali R H, Ghalib B A and Abdoon R S 2019 *7th Int. Conf. on Applied Science and Technology (ICAST 2019)* (Karbala: Iraq/AIP Conf. Proc.) **2144** 030028.
[8] Ghalib B A, Abdulkareem O H and Diam W A 2019 *The 2nd Int. Scientific Conf. (Pure Science, Brilliant Creativity and Renewed Building)* (Karbala: Iraq/IOP Conf. Series: Materials Sci. and Engineering) **571** 012122.
[9] Abd Ali R H, Abdoon R S and Ghalib B A 2019 *The 1st Int. Scientific Conf. on Pure Science (ISCPS 2019),* (Najaf: Iraq/J. of Phys.: Conf. Series) **1234** 012005.
[10] Wang H, Xiang S and Gong J 2019 *Multimed. Tools Appl.* **78** 26181–26201.
[11] Jayaprasath E *et al.* 2019 *Photonics* **6** 49–62.
[12] Xiong X, Shi B, Yang Y, Ge L and Wu J 2020 *Opt. Express* **28** 29064–29075.
[13] Emshary C A, Sultan H A and Hassan R M 2016 *J. Babylon Univ. Appl. Sci.* **24** 1371–1377.
[14] Oleiwi M O, Sultan H A, Hashim D H, Chekheim A M and Emshary C A 2017 *J. Coll. Educ. Pure Sci.* **7** 214–231.
[15] Desmet R and Virte M 2020 *J. Phys. Photonics* **2** 025002.
[16] Mahmoud E E, Higazy M and Al-Harthi T M 2019 *Mathematics* **7** 1–26.
[17] Jayaprasath E, Hou Y S, Wu Z M, and Xia G Q 2018 *IEEE Access* **6** 58482–58490.
[18] Buldú J M, García-Ojalvo J and Torrent M C 2004 *IEEE J. Quantum Electron.* **40** 640–650.
[19] Jiang N, Xue C, Lv Y and Qiu K 2016 *Nonlinear Dyn.* **86** 1937–1949.
[20] Kusumoto K and Ohtsubo J 2003 *IEEE J. Quantum Electron.* **39** 1531–1536.
[21] Buldú J M et al. 2002 *Phys. and Simulation of Optoelectronic Devices X* **4646** 411–419.
[22] Wu J *et al.* 2011 *IEEE PHOTONICS Technol. Lett.* **23** 1854–1856.
[23] Locquet A, Masoller C, Mégret P and Blondel M 2002 *Opt. Lett.* **27** 31–33.
[24] Locquet A, Masoller C and Mirasso C R 2002 *Phys. Rev. E* **65** 056205.
[25] Vicente R, Fischer I and Mirasso C R 2008 *Phys. Rev. E* **78** 066202.
[26] Hammood H A and Sultan H A 2020 *The 8th Int. Conf. on Applied Science and Technology* (ICAST 2020) (Karbala: Iraq/AIP Conf. Proc.) **2290** 050047.